Electromagnetic Modeling of Interconnects for Mixed-Signal Integrated Circuits from DC to Multi-GHz Frequencies

Aosheng Rong and Andreas C. Cangellaris

Center for Computational Electromagnetics, Department of Electrical & Computer Engineering
University of Illinois at Urbana-Champaign, Urbana, IL 61801, U.S.A.

Abstract - **This paper presents a numerically stable methodology for the electromagnetic analysis of three-dimensional interconnect structures from very low (almost dc) to multi-GHz frequencies. The proposed methodology is based on a generalized version of the partial element equivalent circuit interpretation of the electric field integral equation that utilizes triangular cells for the discretization of conductor surfaces and thus is capable of handling structures of arbitrary shapes. The numerical stability of the approximate problem at very low frequencies is achieved through capturing an appropriate tree of the network graph, yielding an enhanced circuit mesh analysis. Numerical experiments are used to demonstrate the numerical stability of the numerical methodology even for frequencies at which the structure under study is a minute fraction of the wavelength.**

I. INTRODUCTION

Broadband electromagnetic analysis of interconnect for mixed-signal integrated circuits is essential for accurate electromagnetic interference prediction in compact, high-density, multi-functional systems aimed toward system-on-a-chip designs. The interconnect and circuit density in such systems is such that all electromagnetic interactions need be taken into account for accurate design. This fact has motivated the trend toward the development of a new breed of electromagnetic CAD tools that can address the complexity of such circuits, while providing the electromagnetic accuracy needed for accurate analysis. Despite their complexity, the mixed-signal nature of their application makes these integrated circuits electrically small over a significant bandwidth of their application. It is well known that standard electromagnetic integral equation solvers become numerically unstable and thus unreliable when applied to the solution of electrically small structures (e.g. [1]-[3]). This difficulty in closely related to the increasing decoupling of the electric and magnetic fields as the frequency tends to zero. In order to highlight one of the aspects of this decoupling, consider the equation $\vec{E} = -j\omega\vec{A} - \nabla\Phi$ that leads to the electric field integral equation (EFIE) formulation of the electromagnetic boundary value problem. Recognizing the fact that the vector potential term is proportional to $j\omega\vec{J}$, while the scalar potential is proportional to $(j\omega)^{-1}\nabla\cdot\vec{J}$, it is clear that the contribution from the vector potential term will be lost in the finite-precision numerical solution of the problem as the frequency tends to zero. As explained in detail in [3], this difficulty can be overcome through a loop-star or loop-tree decomposition of the unknown current distribution, so that the solenoidal (divergence-free) component of the current, responsible for the quasi-static magnetic field, and its complementary (curl-free) component, responsible for the quasi-static electric field, are modeled independently. The two components of the current density exhibit disparate frequency dependency that is instrumental in improving the stability of the numerical solution of the EFIE at very low frequencies while maintaining solution accuracy.

It is shown in this paper that, in the context of the partial element equivalent circuit (PEEC) interpretation of the EFIE [4], the benefits from the loop-tree-like decomposition of the unknown current density can be realized in an alternative and more straightforward fashion, through the re-formulation of the PEEC interpretation of the EFIE in the spirit of an enhanced circuit mesh analysis.

II. MATHEMATICAL FORMULATION

The important attribute of the PEEC formulation of the electromagnetic problem is that leads directly to a description of the electromagnetic problem in terms electromagnetically retarded couplings between the unknown currents and charges in the discrete model that maintain their inductive and capacitive nature familiar from the distributed lumped-circuit representation of electromagnetic effects at low frequencies. Thus the PEEC model can be used for the direct synthesis of equivalent circuit representations of electromagnetic interactions in complex integrated circuits. The PEEC formulation is based in the enforcement of a discrete approximation of the equation for the electric field,

0-7803-7239-5/02/$10.00 © 2002 IEEE

$$\vec{E}(\vec{r}) = -j\omega\vec{A}(\vec{r}) - \nabla\Phi(\vec{r}) \quad (1)$$

through a Galerkin's testing at each and every element in the discrete model of the interconnect structure. In the above equation, $\vec{A}(\vec{r})$ and $\Phi(\vec{r})$ are, respectively, the magnetic vector and electric scalar potentials. Their expressions in terms of Poisson's integrals are well known. In the proposed formulation, polarization currents are introduced to account for the presence of inhomogeneous dielectric volumes. Therefore, the Green's function used in the Poisson's integrals for the potential is the free-space Green's function. Furthermore, a triangular mesh is used for the discretization of conductor surfaces. Dielectric volumes are discretized by means of prisms. Prisms are used also for the discretization of the volume of conductors when a volumetric rather than a surface model is used to account for skin effect. For the case of a surface model for the representation of electric current flow in the conductors, the surface electric current density $\vec{J}$ and the surface electric charge density ρ are expanded, respectively, into the roof-top Rao-Wilton-Glisson (RWG) expansion functions [5], and pulse (piece-wise constant) functions [6]. Use of these expansion functions in conjunction with the Galerkin's testing of the EFIE yields the familiar PEEC statement of the problem (when only conductors are involved),

$$Z_a I_a + \sum_{n=1}^{N} j\omega L_{an} I_n - \sum_{m=1}^{M} p_{\beta m} Q_m + \sum_{m=1}^{M} p_{\gamma m} Q_m = V_a^{(s)} \quad (2)$$

where Z_a is the surface impedance for element a, and the remaining coefficients are given by,

$$L_{an} = \frac{\mu}{4\pi} \iint_{T_a^+ + T_a^-} \vec{f}_a(\vec{r})ds \cdot \iint_{T_n^+ + T_n^-} G_0(\vec{r},\vec{r}')\vec{f}_n(\vec{r}')ds',$$

$$p_{\beta m} = \frac{1}{4\pi\varepsilon_0} \iint_{T_a^+} q_\beta ds \iint_{T_m} G_0(\vec{r},\vec{r}')\, q_m ds', \quad (3)$$

$$p_{\gamma m} = \frac{1}{4\pi\varepsilon_0} \iint_{T_a^+} q_\gamma ds \iint_{T_m} G_0(\vec{r},\vec{r}')\, q_m ds'$$

where G_0 denotes the free-space Green's function, and the source $V_a^{(s)}$ is introduced to account for the excitation. The presence of finite dielectric volumes introduces extra unknowns, associated with the discretization of the bound charge and polarization current density. More specifically, proper expansion functions are used to represent the polarization current density $\vec{J}_d = j\omega(\varepsilon_r - 1)\varepsilon_0\vec{E}$ inside the triangular prisms used for the discretization of the finite dielectrics. These expansion functions may be thought of as the generalization of the roof-top basis functions stated earlier to three dimensions, where the represented transverse current densities are assumed to be constant in the vertical direction, while the vertical component of the current density is assumed constant in the transverse direction and exhibiting a linear (roof-top) function variation in the vertical direction. The details of the PEEC interpretation of the dielectric volume modeling can be found in [6].

In (2) conservation of electric charge has not been enforced. In the spirit of PEEC the enforcement of this condition is interpreted as the generalized form of Kirchhoff's current law. Let $\mathbf{V}_{bl}$ denote the vector of "voltages" across the "inductive" branches in the PEEC circuit, $\mathbf{V}_{bp}$ the vector of the "voltages" at the "capacitive" nodes, while the vectors $\mathbf{I}_{bl}$ and $\mathbf{I}_{bp}$ contain the corresponding currents, respectively. The vector of unknown charges is related to $\mathbf{I}_{bp}$ through $j\omega\mathbf{Q}_p = \mathbf{I}_{bp}$. The combination of the discrete form of the conservation of charge equation with (2) yields the complete form of the PEEC approximation of the electromagnetic problem, which may be cast in matrix form as follows,

$$\begin{bmatrix} \mathbf{Z}_S + j\omega\mathbf{L} & \mathbf{0} \\ \mathbf{0} & (j\omega)^{-1}\mathbf{P} \end{bmatrix} \begin{bmatrix} \mathbf{I}_{bl} \\ \mathbf{I}_{bp} \end{bmatrix} = \begin{bmatrix} \mathbf{V}_{bl} \\ \mathbf{V}_{bp} \end{bmatrix} \quad (4)$$

This is typically referred to as the nodal analysis PEEC model [4], and its matrix properties are identical to those of the method of moments matrix obtained for the EFIE using a Galerkin's approach with the RWG as the expansion and testing functions. Hence, it also exhibits the low-frequency ill-conditioning mentioned in the Introduction. This ill-conditioning, in the context of PEEC, has also been reported in [7]. It was noted in [7] that, contrary to the above nodal analysis formulation of the discrete problem, a mesh analysis yields a more stable discrete system at low frequencies. In view of the discussion in the Introduction of the effective use of the loop-star decomposition of the current density to improve the low-frequency numerical stability of the approximation, the improvement obtained by the application of mesh analysis makes sense. At the same time it motivates a systematic methodology for the transformation of the discrete problem of [4] into one that is free from low-frequency numerical instability. This methodology is outlined in the following.

Once the discrete PEEC model has been generated, application of mesh analysis requires the identification of all independent loops in the network graph that describes the discrete model. Associated with these loops is a loop matrix **M**. The identification of the loops requires the selection of a tree first. The proposed procedure makes the selection of the tree for the network that results after all

"capacitive" branches are opened. Hence, the independent loops obtained from this tree contain only "inductive" branches. Subsequently, the "capacitive" branches are re-introduced in the network and the remaining independent loops are identified.

Once all independent loops have been identified, the mesh currents associated with these loops become the new unknown quantities. Let $\mathbf{I}_m$ be the vector of the mesh currents. The branch currents are obtained from it through the mapping, $\mathbf{I}_b = \mathbf{M}^T \mathbf{I}_m$. The loop matrix $\mathbf{M}$ can be used to express in a discrete form Faraday's law for each one of the loops. More specifically, it is,

$$\mathbf{M}\begin{bmatrix}\mathbf{V}_{bl}\\ \mathbf{V}_{bp}\end{bmatrix} = \mathbf{V}_S \qquad (5)$$

where the vector, $\mathbf{V}_S$, of external voltage source terms has been identified explicitly. Clearly, (5) and the relationship between mesh currents and branch currents given above, can be utilized in (4) to recast the discrete PEEC model in the following form,

$$\left(\mathbf{M}_{bl}(\mathbf{Z}+j\omega\mathbf{L})\mathbf{M}_{bl}^T + (j\omega)^{-1}\mathbf{M}_{bp}\mathbf{P}\mathbf{M}_{bp}^T\right)\mathbf{I}_m = \mathbf{V}_S \qquad (6)$$

This completes the development of the alternative, mesh analysis-based formulation of the PEEC interpretation of the EFIE statement of the electromagnetic problem. Its superior numerical stability as the operating frequency tends to zero is demonstrated through its application to the electromagnetic analysis of simple interconnect structures.

II. Numerical Experiments

The first numerical example considers the electromagnetic modeling of a perfectly conducting rectangular strip of length 2.5mm and width 0.25mm. The strip is assumed to be of zero thickness. Voltage sources are connected at the two ends of the strip (see Fig. 1), for the purposes of obtaining the two-port admittance parameters of the strip. Clearly, the self admittance Y_{11} represents the input admittance seen at port 1 with port 2 shorted. Hence, it is expected to exhibit a purely inductive performance, i.e., $Y_{11}(\omega) = -(j\omega L_S)^{-1}$ at very low frequencies. Fig. 1 depicts the frequency variation of Y_{11} over the bandwidth 10 MHz – 10 GHz. It is noted that while the standard method of moments solution fails to capture the anticipated inductive behavior, the mesh analysis-based PEEC model captures this behavior successfully. This is further demonstrated through the extraction of the self inductance of the rectangular strip from the calculated values of Y_{11} at 10 Hz, 10 KHz, and 10 MHz. As Table I demonstrates, excellent agreement is observed with the closed-form expression for the self inductance obtained from [8].

The second example considers the 4x4 interconnect prototype shown in Fig.2. The dimensions of the interconnects are as L_x=750μm,w_{x1}=w_{x2}=w_{x3}=w_{x4}=40μm, s_{x1}=s_{x2}=s_{x3}=40μm, Ly=680μm, d=50μm. w_{y1}=w_{y2}=50μm, w_{y3}=w_{y4}=50μm, and s_{y1}=s_{y2}=s_{y3}=50μm. Fig.3 and Fig.4 depict a representative set of admittance parameters and scattering parameters, respectively, over the frequency range 1 kHz to 10 GHz. The ripple behavior in the plots of the scattering parameters at very low frequencies is attributed to numerical noise since at such frequencies the coupling between crossing lines is so weak that may be considered zero for all practical purposes.

V. Conclusion

In conclusion a systematic methodology has been presented for the broadband electromagnetic analysis of interconnect structures from dc to multi-GHz frequencies. Such broadband analysis is essential for the design and performance verification of highly-integrated, mixed-signal circuits, of the type encountered in system-in-a-package and system-on-a-chip designs. The proposed methodology overcomes the numerical instabilities present in the integral equation formulations of the electromagnetic problem when the electrical size of the structure becomes a very small fraction of the operating wavelength. Thus, a rigorous and highly accurate analysis of the electromagnetic behavior of the interconnect structure become possible across the entire frequency spectrum, as demonstrated by the numerical experiments.

Acknowledgement

This work was supported in part by Intel Corporation through a grant to the ECE Department, University of Illinois at Urbana-Champaign.

References

[1] D. R. Wilton and A. W. Glisson, "On improving the electric field integral equation at low frequencies," *Proc. URSI Radio Science Meeting*, Los Angeles, CA, Jun. 1981.

[2] W. Wu, A. W. Glisson, and D. Kajfez, "A study of two numerical solution procedures for the electric field integral equation at low frequency," *Appl. Computat., Electromag. Soc. J.*, vol. 10, no. 3, pp. 69-80, Nov. 1995.

[3] J.-S. Zhao and W. C. Chew, "Integral equation solution of Maxwell's equations from zero frequency to microwave frequencies," *IEEE Trans. Antennas, Propagat.*, vol. 48, no. 10, pp. 1635-1645, Oct. 2000.

[4] A. Ruehli, "Equivalent circuit models for three-dimensional multiconductor systems," *IEEE Trans. Microwave Theory Tech.*, vol. MTT-22, pp. 216-221, Mar. 1974.

[5] S. M. Rao, D. R. Wilton, and A. W. Glisson, "Electromagnetic scattering by surfaces of arbitrary shape," *IEEE Trans. Antennas Propagat.*, vol. AP-30, pp. 409-418, May 1982.

[6] A. Rong and A. C. Cangellaris, "Generalized PEEC models for three-dimensional interconnect structures and integrated passives of arbitrary shapes," *Proc. IEEE Topical Meeting on Electrical Performance of Electronic Packaging*, Boston, MA, October 2001.

[7] M. Kammon, N. A. Marques, L. M. Silveira, and J. White, "Automatic generation of accurate circuit models of 3-D interconnect," *IEEE Trans. Comp. Pack. & Manufacturing Tech. – Part B*, Vol. 21, no. 3, pp. 225-234, Aug. 1998.

[8] C. Paul, *Principles of Electromagnetic Compatibility*. Wiley, New York, 1992.

Table I Self partial inductance for a single conductor

PEEC+Mesh Analysis				Explicit Formula [8]
Frequency	10Hz	10KHz	10MHz	
Ls (nH)	1.764276	1.764276	1.764277	1.764325

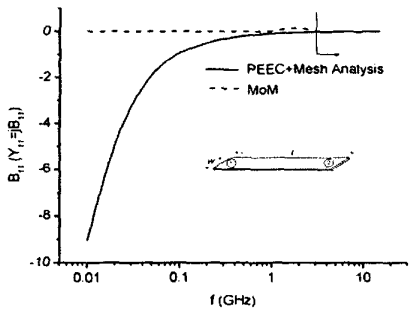

Figure 1. Admittance parameter Y_{11} of a strip.

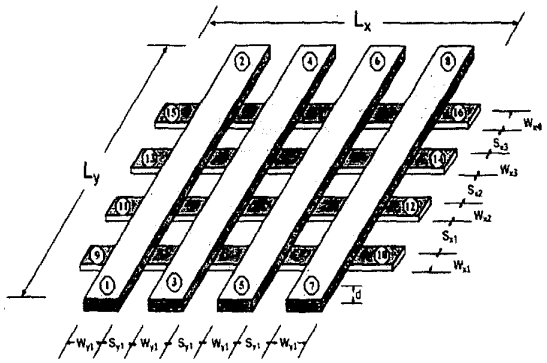

Figure 2. 4x4 on-chip interconnect crossover.

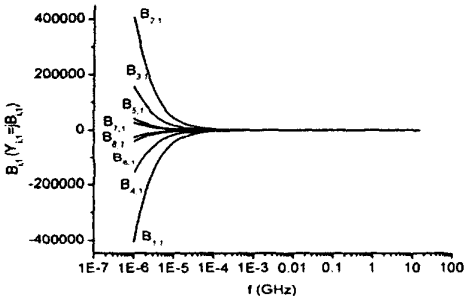

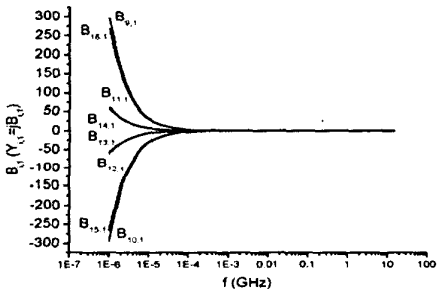

Figure 3. Admittance parameters $Y_{i,1}$ for the 4x4 interconnect crossover.

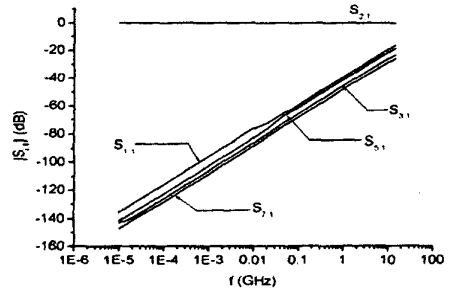

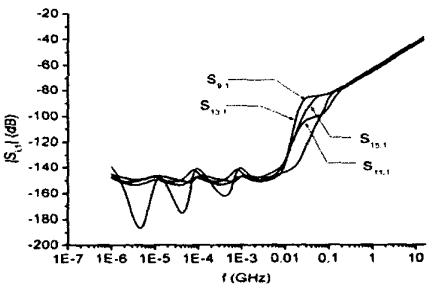

Figure 4. Scattering parameters $S_{i,1}$ for the 4x4 interconnect crossover.